ACS Catalysis

Research Article

pubs.acs.org/acscatalysis

Tailorable Synthesis of Porous Organic Polymers Decorating Ultrafine Palladium Nanoparticles for Hydrogenation of Olefins

Liuyi Li,[†,‡] Huaixia Zhao,[†,‡] and Ruihu Wang*[,†,‡]

[†]State Key Laboratory of Structural Chemistry, Fujian Institute of Research on the Structure of Matter, Chinese Academy of Sciences, Fuzhou, Fujian 350002, China

[‡]Key Laboratory of Coal to Ethylene Glycol and Its Related Technology, Chinese Academy of Sciences, Fuzhou, Fujian 350002, China

Supporting Information

ABSTRACT: Two 1,2,3-triazolyl-containing porous organic polymers (CPP-C and CPP-Y) were readily synthesized through click reaction and Yamamoto coupling reaction, respectively. The effects of synthetic methods on the structures and properties of CPP-C and CPP-Y were investigated. Their chemical compositions are almost identical, but their physical and texture properties are different from each other. Ultrafine palladium nanoparticles can be effectively immobilized in the interior cavities of CPP-C and CPP-Y. The interactions between polymers and palladium are verified by IR, solid-state NMR, XPS, and EDS. Their catalytic performances are evaluated by hydrogenation of olefins. Pd@CPP-Y exhibits higher catalytic activity and recyclability than Pd@CPP-C. Hot filtration and the three-phase test indicate that hydrogenation functions in a heterogeneous pathway.

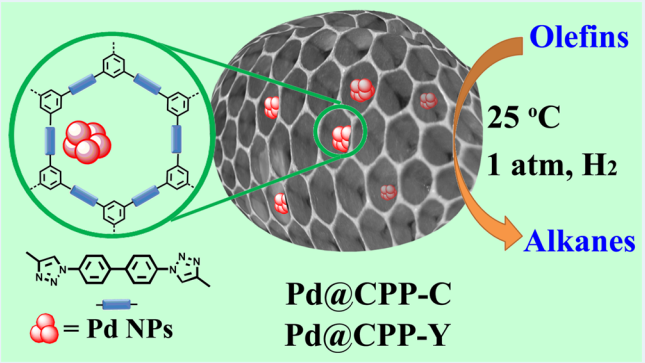

KEYWORDS: *click reaction, porous organic polymers, palladium nanoparticles, heterogeneous catalysis, hydrogenation*

1. INTRODUCTION

The synthesis of supported metal nanoparticles (NPs) has attracted considerable attention because of their potential applications in energy conversion, environmental remediation, and catalysis.[1,2] Ultrafine metal NPs usually exhibit unique properties distinct from those in large-size NPs and bulk metal counterparts and are thought to be more reactive in catalysis,[3−5] but they are prone to aggregate during catalytic reactions owing to high surface energy, leading to the loss of catalytic activity.[6,7] By serving as unique host matrices, MOFs have been reported to be a family of ideal supports for the immobilization and stabilization of ultrafine metal NPs,[8−10] which results in catalytic systems with high selectivities and catalytic activities.[11−13] However, the reversible nature of metal-coordination chemistry usually makes them unstable enough in most liquid-phase catalysis. Taking into account the similarity to MOFs, porous organic polymers (POPs) also can serve as a promising platform for incorporating metal NPs within the pores of POPs.[14−21] Spatial control of catalytically active sites in POPs can be tuned and modified through vast choice of organic building blocks and synthetic diversity, which endows them potential for catalysis.[22−24] Generally, the porous structure of POPs plays an important role in catalysis,[25] which is highly dependent on the geometry and size of monomers as well as the synthetic method of POPs.[26−29] The intensive efforts have been focused on the construction of functionalized POPs by judicious selection of building blocks, in which functional groups, such as triazolyl, imine, urea, and salen, not only can serve as linkages of POPs but also are favorable for stabilization of metal ions and NPs.[30−33] For example, a two-dimensional imine-based POF (Pd/COF-LZU1) has been reported to support palladium ions and NPs through the confinement of polymer and coordination of imine to palladium, and excellent catalytic activity and recyclability were shown in the Suzuki−Miyaura coupling reaction.[34] However, studies on the effects of synthetic methods on the structures, properties, and applications of target POPs are rare.[35]

Click reaction of organic azides and terminal alkynes has become a common coupling procedure in many interdisciplines owing to its superior reliability and modular synthesis.[36−38] Recently, several 1,2,3-triazoyl-containing POPs have been prepared through click reaction[39,40] and have been explored as sorbents for gas storage[41−43] and supports of metal nanoparticles (NPs) for heterogeneous catalysis.[21,44,45]It is known that homocoupling reactions of rigid monomers are more controllable than cross-coupling reactions. Nickel-mediated Yamamoto coupling reaction is one of the efficient methods for

Received: July 7, 2014
Revised: December 25, 2014
Published: December 28, 2014

DOI: 10.1021/cs501731w
ACS Catal. 2015, 5, 948−955

aryl−aryl homocoupling of aryl-halogenide compounds.[46] Several POPs with high surface area have been synthesized through Yamamoto coupling reaction.[47−52] Among them, PAF-1 and PPN-4, which were prepared by self-condensation of tetrakis(4-bromophenyl)methane and tetrakis(4-bromophenyl)silane, respectively, possess the ultrahigh BET surface area of 5640 and 6461 $m^2\ g^{-1}$, respectively.[53,54] As a result, it will be interesting to compare the performances of 1,2,3-triazoyl-containing POPs from click cross-coupling reaction and Yamamoto homocoupling reaction. As a continuation of our studies in click-based porous organic polymers (CPPs),[21,49] herein, we report the effects of synthetic methods on the structures and properties of 1,2,3-triazoyl-containing POPs, CPP-C and CPP-Y, which were synthesized via click reaction and Yamamoto coupling reaction, respectively. In comparison with CPP-C, CPP-Y exhibits superior performances in gas sorption, immobilization of ultrafine palladium nanoparticles (NPs), and hydrogenation of olefins.

2. EXPERIMENTAL SECTION

General Information. 1-Azido-4-bromobenzene,[55] 4,4′-diazidobiphenyl,[55] 1,3,5,-triethynylbenzene,[56] Merrifield resin supported 5-hexen-1-ol, and Merrifield resin supported 1-hexanol[57] were prepared according to literature methods. Other chemicals were commercially available and used without further purification. ^{1}H and ^{13}C NMR spectra were recorded on a Bruker AVANCE III NMR spectrometer at 400 and 100 MHz, respectively, using tetramethylsilane (TMS) as an internal standard. Solid-state ^{13}C CP/MAS NMR was performed on a Bruker SB Avance III 500 MHz spectrometer with a 4 mm double-resonance MAS probe. IR spectra were recorded with KBr pellets using PerkinElmer Instrument. Raman spectra were recorded on a Renishaw inVia system by using 633 nm laser. Thermogravimetric analysis (TGA) was carried out on NETZSCH STA 449C by heating samples from 30 to 700 °C in a dynamic nitrogen atmosphere with a heating rate of 10 °C·min^{-1}. Powder X-ray diffraction (XRD) patterns were recorded in the range of 2θ = 5−85° on a desktop X-ray diffractometer (RIGAKU-Miniflex II) with Cu Kα radiation (λ = 1.5406 Å). Nitrogen adsorption and desorption isotherms were measured at 77 K using a Micromeritics ASAP 2020 system, and the samples were degassed at 100 °C for 10 h before the measurements. Surface areas were calculated from the adsorption data using Brunauer−Emmett−Teller (BET). The pore size distribution curves were obtained from the adsorption branches using nonlocal density functional theory (NLDFT) method. Field-emission scanning electron microscopy (SEM) was performed on a JEOL JSM-7500F operated at an accelerating voltage of 3.0 kV. Transmission electron microscope (TEM) images were obtained on TECNAI G^2 F20. X-ray photoelectron spectroscopy (XPS) measurements were performed on a Thermo ESCALAB 250 spectrometer, using nonmonochromatic Al Kα X-rays as the excitation source and choosing C 1s (284.6 eV) as the reference line. Inductively coupled plasma spectroscopy (ICP) was measured on Jobin Yvon Ultima2. Gas chromatography (GC) was performed on a Shimadzu GC-2014 equipped with a capillary column (RTX-5, 30 m × 0.25 μm) using a flame ionization detector. Elemental analyses were performed on an Elementar Vario MICRO Elemental analyzer.

Synthesis of 1,3,5-Tris(1-(4-bromophenyl)-1H-1,2,3-triazol-4-yl)benzene. Sodium ascorbate (120 mg, 0.6 mmol) was added to a suspension of 1-azido-4-bromobenzene (790 mg, 4.0 mmol), 1,3,5,-triethynylbenzene (150 mg, 1.0 mmol), and $CuSO_4{\cdot}5H_2O$ (75 mg, 0.3 mmol) in *t*-BuOH/H_2O (10/10 mL). The reaction mixture was stirred at room temperature for 24 h. The precipitate was isolated by filtration and washed successively with H_2O (20 mL) and methanol (10 mL). The crude product was further purified by flash column chromatography on silica gel using cyclohexane/CH_2Cl_2 (2:1) as eluent to give target product as a yellow solid. Yield: 0.3 g (40%). ^{1}H NMR (400 MHz, DMSO-*d*6): δ 9.50 (s, 3H), 8.54 (s, 3H), 8.20−8.65 (m, 12H); ^{13}C NMR (100 MHz, DMSO-*d*6): δ 146.7, 136.2, 133.4, 131.9, 122.3, 121.9, 121.0; IR (KBr, cm^{-1}): 3097 (w), 2970 (vw), 2335 (vw), 2271 (vw), 1897 (vw), 1615 (w), 1497 (vs), 1395 (m), 1320 (w), 1233 (m), 1074 (m), 1039 (s), 1014(m), 986 (s), 882 (w), 825 (s), 781 (m), 719 (w), 507 (vw).

Synthesis of CPP-C. To a solution of 4,4′-diazidobiphenyl (0.58 g, 2.4 mmol), $CuSO_4{\cdot}5H_2O$ (120 mg, 0.5 mmol) and 1,3,5,-triethynylbenzene (0.24 g, 1.6 mmol) in DMF (100 mL), sodium ascorbate (95 mg, 0.5 mmol) was added under N_2 atmosphere. The stirring mixture was heated to 100 °C and maintained at the temperature for 3 days. The precipitate was isolated by filtration, rinsed with DMF (2 × 30 mL) and methanol (2 × 30 mL), and then redispersed in saturated EDTA-2Na solution (20 mL) at room temperature for 12 h. After the solution was filtered and washed with excess H_2O and methanol, the resultant material was purified by Soxhlet extraction using THF, dried in vacuo at 80 °C for 12 h to afford CPP-C as a brown powder. Yield: 0.68 g (83%). IR (KBr, cm^{-1}): 3402 (m), 3137 (w), 3058 (w), 2926 (vw), 2097 (w), 1608 (s), 1506 (vs), 1458 (vw), 1399 (m), 1328 (vw), 1231 (m), 1108 (w), 1042 (s), 988 (m), 883 (w), 825 (s), 779 (m), 528 (w); Anal. Calcd (%) for $(C_{10}H_6N_3)_n$: C, 71.42; H, 3.60; N, 24.99. Found: C, 65.25; H, 4.64; N, 20.62.

Synthesis of CPP-Y. To a solution of bis(1,5-cyclooctadiene)-nickel(0) (1.6 g, 5.8 mmol) and 2,2′-bipyridyl (0.9 g, 5.8 mmol) in dehydrated DMF (40 mL), 1,5-cyclooctadiene (0.6 g, 5.8 mmol) was added, and the mixture was heated at 80 °C for 1 h. 1,3,5-Tris(1-(4-bromophenyl)-1H-1,2,3-triazol-4-yl)-benzene (1.2 g, 1.6 mmol) in dehydrated DMF (60 mL) was added to the resultant purple solution at 80 °C. The mixture was stirred at 80 °C for 3 days to obtain the deep purple suspension. After cooling to room temperature, the concentrated HCl was added to the mixture until it turned to a green suspension. After filtration, the residue was washed with H_2O (2 × 30 mL) and then redispersed in saturated EDTA solution (20 mL) at room temperature for 3 h. After filtered and washed with excess H_2O and methanol, the resultant material was purified by Soxhlet extraction using THF, dried in vacuo at 80 °C for 12 h to afford CPP-Y as a brown powder. Yield: 0.69 g (81%). IR (KBr, cm^{-1}): 3428 (m), 2967 (w), 2927 (w), 2345 (w), 1608 (s), 1504 (vs), 1385 (m), 1321 (vw), 1228 (m), 1106 (vw), 1042 (s), 988 (w), 883 (vw), 825 (m), 780 (w), 530 (vw); Anal. Calcd (%) for $(C_{10}H_6N_3)_n$: C, 71.42; H, 3.60; N, 24.99. Found: C, 60.17; H, 4.66; N, 20.12.

Synthesis of Pd@CPP-C and Pd@CPP-Y. To a solution of $Pd(OAc)_2$ (81 mg, 0.36 mmol) in dichloromethane (100 mL), CPP-C or CPP-Y (200 mg) was added. After stirring at 60 °C for 24 h, the precipitate was isolated by filtration. The resultant solid was purified by Soxhlet extraction with dichloromethane, dried in vacuo at 80 °C for 12 h to give a brown solid, and then reduced in a stream of H_2/N_2 (10% H_2, 100 mL/min^{-1}) at 200 °C for 4 h to afford Pd@CPP-C and Pd@CPP-Y. Pd contents

DOI: 10.1021/cs501731w
ACS Catal. 2015, 5, 948−955

Scheme 1. Synthesis of CPP-C and CPP-Y as well as Schematic Illustration of Pd@CPP-C and Pd@CPP-Y

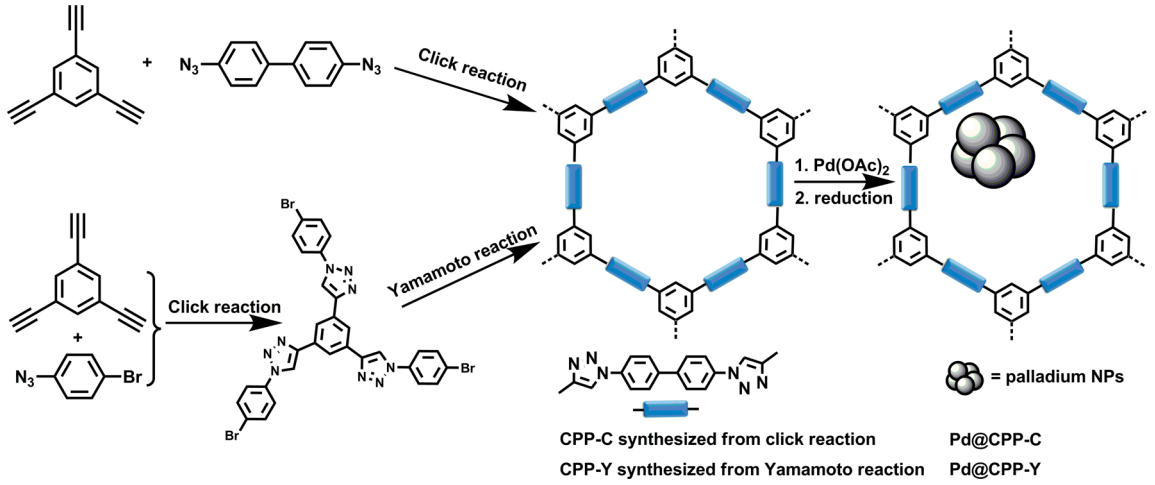

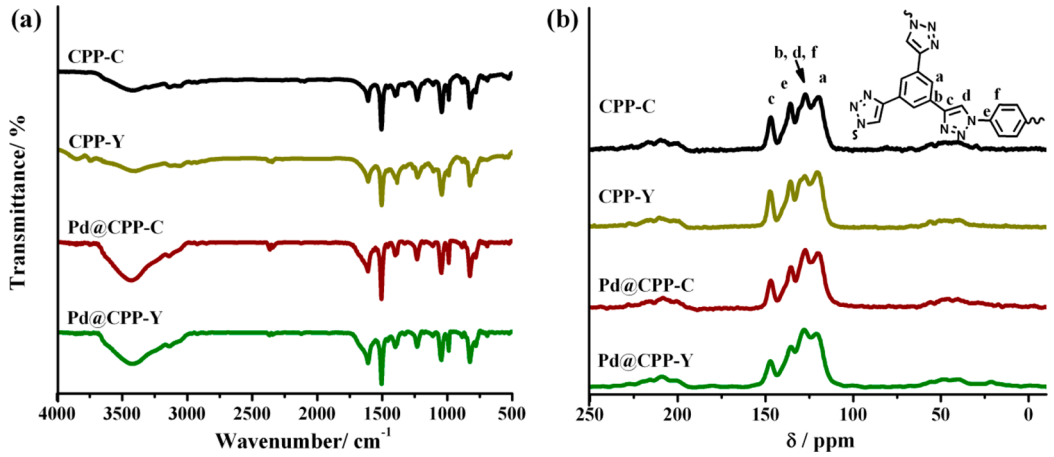

Figure 1. IR spectra (a) and solid-state ^{13}C NMR spectra (b) for CPP-C, CPP-Y, Pd@CPP-C, and Pd@CPP-Y.

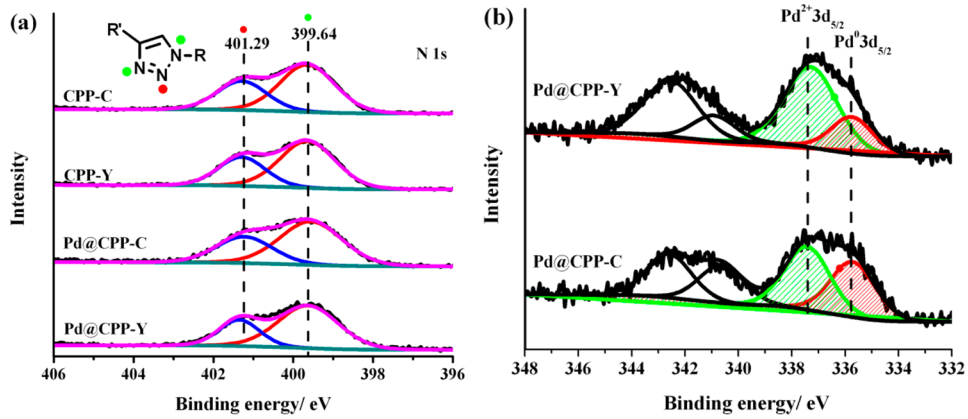

Figure 2. XPS spectra of N 1s for CPP-C, CPP-Y, Pd@CPP-C and Pd@CPP-Y (a), and Pd 3d for Pd@CPP-C and Pd@CPP-Y (b).

in Pd@CPP-C and Pd@CPP-Y were determined by ICP analysis, they are 0.386 and 0.645 mmol g^{-1}, respectively.

Hydrogenation of Olefin. A high-pressure reactor was charged with olefin (2 mL) and Pd@CPP-C or Pd@CPP-Y (1/5000 equiv of Pd per olefin mol) in ethanol (2 mL). The reactor was sealed and purged with hydrogen at 0 °C to remove air. Hydrogen was introduced into the reactor at the constant pressure, the reactor was placed into the preheated oil bath with the agitation speed 1000 rpm. After a suitable reaction time, the reactor was placed in ice water and gas was released. The products were analyzed using GC. The structures of the products were confirmed by comparison with GC retention time of commercial materials and literature NMR spectroscopic data. Solvent-free hydrogenation was carried out following the same method described above except the absence of ethanol.

Recyclability Test for Hydrogenation of Olefin. After hydrogenation of neat 1-hexene, the liquid was isolated by decantation. After washing twice with *n*-hexane and drying in

DOI: 10.1021/cs501731w
ACS Catal. 2015, 5, 948−955

vacuo at room temperature for 0.5 h, the recovered gray solid was reused directly for the next run.

3. RESULTS AND DISCUSSION

Following the synthetic route outlined in Scheme 1, CPP-C was readily prepared by copper-catalyzed click reaction of 1,3,5-triethynylbenzene with 4,4′-diazidobiphenyl, whereas CPP-Y was synthesized by click reaction of 1,3,5-triethynylbenzene and 4-bromophenyl azide, followed by nickle-mediated Yamamoto coupling reaction. Both CPP-C and CPP-Y are brown powders, and they are insoluble in water and common organic solvents.

IR, solid-state ^{13}C NMR, and XPS spectra of CPP-C and CPP-Y are close to each other, owing to their similar chemical structure. In the IR spectrum of CPP-C, the formation of the 1,2,3-triazolyl linkage is clearly confirmed by the disappearance of characteristic peaks of terminal alkynyl and azide groups at 3281 and 2112 cm^{-1}, respectively, and the concomitant emergence of characteristic peaks of 1,2,3-triazolyl group at 1610 and 3133 cm^{-1} (Figure S1a).[40] The preservation of characteristic peaks of 1,2,3-triazolyl group and the absence of C−Br peak at 1073 cm^{-1} in the IR spectrum of CPP-Y show successful homocoupling of 1,3,5-tris(1-(4-bromophenyl)-1,2,3-triazol)benzene (Figure S1b).[39] In solid-state ^{13}C NMR spectra of CPP-C and CPP-Y, the peak at 147 ppm is ascribed to C4 carbon of 1,2,3-triazolyl ring, and the broad signals at 110−140 ppm correspond to aromatic carbon atoms (Figure 1b).[42] XPS survey spectra show the presence of C, N, and O in CPP-C and CPP-Y (Figure S2). The N 1s regions of CPP-C and CPP-Y are deconvoluted into two peaks. One peak around 401.29 eV is ascribed to N2 atom of 1,2,3-triazolyl, and the other peak around 399.64 eV corresponds to N1 and N3 atoms (Figure 2a).[58,59] Their intensity ratio of the relative peak areas is close to 1:2, which is the same as the ratio of nitrogen content in 1,2,3-triazolyl ring. Elemental analyses of CPP-C and CPP-Y show that the experimental values of C and N are slightly lower than the corresponding theoretical values. The deviations are mainly ascribed to the inclusion of guest molecules in the POPs,[39,60] which is further confirmed by weight loss before 120 °C in TGA curves (Figure S3). XRD analyses reveal CPP-C and CPP-Y are amorphous due to kinetic irreversibility of reaction processes (Figure S4). SEM spectra show that they are composed of granular particles. The particle size of CPP-Y is in the range of 100−300 nm, which is larger than that in CPP-C (below 100 nm) (Figure S5).

The porosities of CPP-C and CPP-Y were investigated by N_2 adsorption/desorption at 77 K. As shown in Figure S6, the isotherm for CPP-Y shows rapid N_2 uptake at low relative pressure (P/P_0 < 0.1), which is typical for microporous materials. The hysteresis is probably attributed to deformation and/or swelling of the polymer at 77 K by N_2.[61] CPP-C exhibits similar isotherm shape, but its gas uptakes at low relative pressures are drastically reduced. BET surface area of CPP-C and CPP-Y are 156 and 408 $m^2\ g^{-1}$, respectively, and their total pore volumes are 0.19 and 0.25 $cm^3\ g^{-1}$, respectively. Interestingly, appreciable amounts of CO_2 adsorption were also observed, owing to the combination of microporous character and nitrogen-rich 1,2,3-triazolyl group in the polymers. CO_2 capture amounts at 273 K and 1 atm in CPP-C and CPP-Y are 70.2 and 87.5 mg g^{-1}, respectively. The isosteric heat of adsorption (Q_{st}) at low coverage of CPP-C and CPP-Y are 34.2 and 28.7 kJ mol^{-1}, respectively, suggesting the binding affinity of CO_2 with the nitrogen-rich polymers (Figure S6c and S6d).[43] CPP-C shows a slightly higher Q_{st} than CPP-Y at the zero coverage, which can be attributed to smaller micropore size of CPP-C than CPP-Y.[35] CPP-Y gives 3.52 mmol g^{-1} H_2 adsorption at 1.1 bar and 77 K, higher than the value of 2.89 mmol g^{-1} found in CPP-C (Figure S6e), which is correlated directly with the surface area and microporous volume of CPP-Y and CPP-C.[39]

Considering the confinement of POPs and coordination ability of 1,2,3-triazolyl moieties,[32,34,62−64] palladium NPs inside CPP-C and CPP-Y were investigated. As shown in Scheme 1, the facile treatment of CPP-C and CPP-Y with palladium acetate in dichloromethane and subsequent reduction in a stream of H_2/N_2 gave rise to gray Pd@CPP-C and Pd@CPP-Y, respectively. Transmission electron microscope (TEM) images show ultrafine palladium NPs are uniformly distributed in Pd@CPP-C and Pd@CPP-Y (Figure 3), and

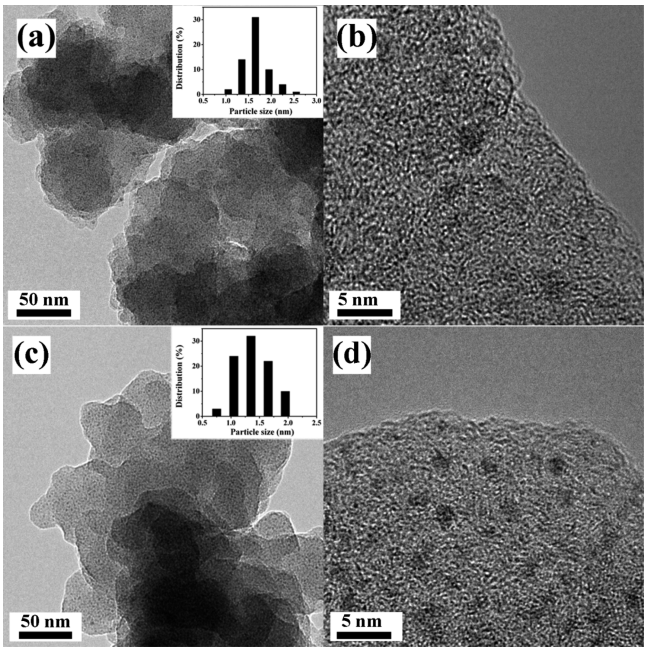

Figure 3. TEM images for Pd/CPP-C (a, b) and Pd/CPP-Y (c, d).

their average sizes are 1.69 ± 0.33 and 1.39 ± 0.31 nm, respectively, which are small enough to be accommodated in the interior cavities of CPP-1 and CPP-2. No obvious characteristic peaks of palladium NPs were observed in XRD patterns of Pd@CPP-C and Pd@CPP-Y, revealing that the particles are too small and/or well dispersed in the polymers (Figure S4). EDS analyses exhibit that Pd@CPP-C and Pd@CPP-Y are composed of C, N, O, and Pd (Figure S7). ICP analyses show Pd contents in Pd@CPP-C and Pd@CPP-Y are 0.386 and 0.645 mmol g^{-1}, respectively. The palladium loading in CPP-C and CPP-Y is in good agreement with their surface area.

In solid-state ^{13}C NMR spectra of Pd@CPP-C and Pd@CPP-Y, signals of aromatic carbons at 110−150 ppm are similar to those in CPP-C and CPP-Y, confirming the integrity of their backbone after palladium loading (Figure 1). In XPS spectra, the appearance of characteristic binding energy peaks of Pd 3d further confirms successful incorporation of palladium (Figure S2). Pd 3d spectra present two sets of doublet peaks corresponding to Pd $3d_{5/2}$ and Pd $3d_{3/2}$. Pd $3d_{5/2}$ peaks at 335.72 and 335.75 eV are attributed to Pd^0 species in Pd@CPP-C and Pd@CPP-Y, respectively, while the peaks at 337.41

DOI: 10.1021/cs501731w
ACS Catal. 2015, 5, 948−955

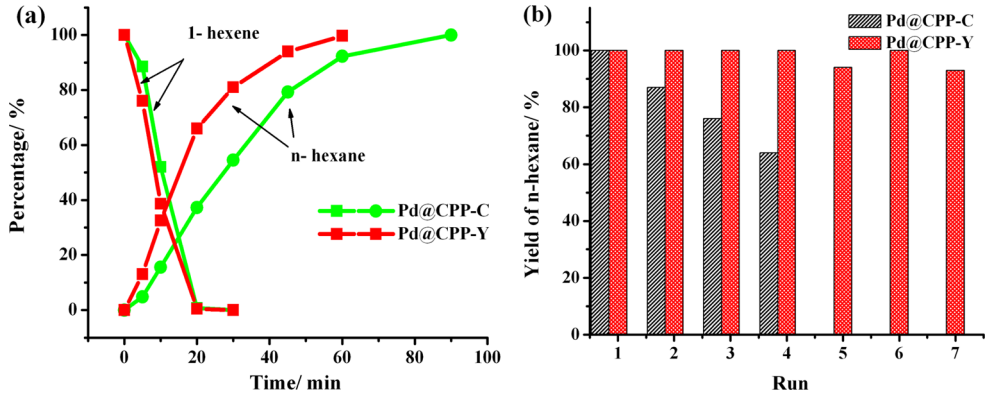

Figure 4. (a) Kinetic profiles of 1-hexene conversion and *n*-hexane formation for Pd@CPP-C and Pd@CPP-Y, (b) reusability of Pd@CPP-C and Pd@CPP-Y. Reaction conditions: the molar ratio of 1-hexene to Pd is 5000, 1.0 atm of H_2, 25 °C, 2 h.

and 337.28 eV are related to Pd^{2+} species in Pd@CPP-C and Pd@CPP-Y, respectively (Figure 2b). The ratios of Pd^0/Pd^{2+} in Pd@CPP-C and Pd@CPP-Y are 0.86 and 0.36, respectively. In comparison with N 1s XPS spectra of CPP-C and CPP-Y, a slight upshift of N 1s characteristic peaks in N 1s XPS spectra of Pd@CPP-C and Pd@CPP-Y was observed, owing to the weak coordination of nitrogen atoms to palladium (Figure 2a). BET surface areas for Pd@CPP-C and Pd@CPP-Y are decreased to 43 and 70 $m^2\ g^{-1}$, respectively, and their total pore volumes are lowered to 0.11 and 0.07 $cm^3\ g^{-1}$, respectively (Figure S6a and S6b). The considerable decrements in BET surface area and pore volumes as well as the increment of pore width have further demonstrated successful incorporation of palladium NPs in the interior cavities of the polymers.[65−67] Despite the significant decrement in surface area and pore volume, Pd@CPP-C and Pd@CPP-Y show hydrogen uptake of 2.10 and 1.87 mmol g^{-1}, respectively.[18,68]

It is known that ultrafine palladium NPs possess a high surface-to-volume ratio and provide a large number of available active sites per unit area for substrates in catalysis. As a result, ultrafine palladium NPs are thought to be more reactive than bulk palladium.[69,70] The catalytic performances of Pd@CPP-C and Pd@CPP-Y were initially investigated by using hydrogenation of neat 1-hexene under 1 atm of H_2 at 25 °C with a olefin/Pd molar ratio of 5000. As shown in Figure 4, kinetic profiles of hydrogenation of 1-hexene show that Pd@CPP-C and Pd@CPP-Y present high conversion in 30 min. A full selectivity of *n*-hexane was achieved after 90 and 60 min in Pd@CPP-C and Pd@CPP-Y, respectively. Not all of the 1-hexene is simultaneously transformed into *n*-hexane, which was attributed to the inherent competition between isomerization and hydrogenation of 1-hexene by using palladium NPs (Figure S8).[71,72] From the proposed mechanism in Scheme S1, the olefin-palladium intermediate can either undergo a reductive elimination to form hexane or *β*-H elimination to form hexene isomers. The surface hydrogen species on palladium play a crucial role in hydrogenation and isomerization of alkenes, but only volume-absorbed hydrogen atoms are prone to react with the olefin-palladium intermediate to form alkane.[73] The faster rate of isomerization than hydrogenation during the early stages of the reaction is a natural consequence of the fact that hydrogen atoms have to diffuse from the surface into the cluster volume. The kinetic profiles of the conversion of 1-hexene as well as the formation of intermediated products and *n*-hexane indicate that ultrafine palladium NPs in Pd@CPP-Y show a higher selectivity for hydrogenation over isomerization than that in Pd@CPP-C and commercial Pd@C, suggesting that the diffusion of hydrogen from the surface into the cluster of the palladium particles can be facilitated by using ultrafine palladium NPs.

The catalytic recyclabilities of Pd@CPP-C and Pd@CPP-Y were also evaluated. For Pd@CPP-C, an obvious decrement of catalytic activity was observed in the consecutive reactions. For examples, the yields of *n*-hexane were decreased to 87% and 64% in the second and fourth runs, respectively. However, Pd@CPP-Y could be used at least seven times without significant loss of catalytic activity. To explore the difference of the two catalytic systems, the resultant powders containing palladium species were isolated after the consecutive reaction and were examined by TEM. As shown in Figure 5, a certain degree of aggregations of palladium NPs on the external surface of Pd@CPP-C and Pd@CPP-Y were observed after the fourth run and the seventh run, respectively, whereas the sizes in the majority of the particles are slightly larger than that in fresh samples. These observations indicate that 1,2,3-triazoyl on the surface of polymers cannot completely prevent the aggregation of external

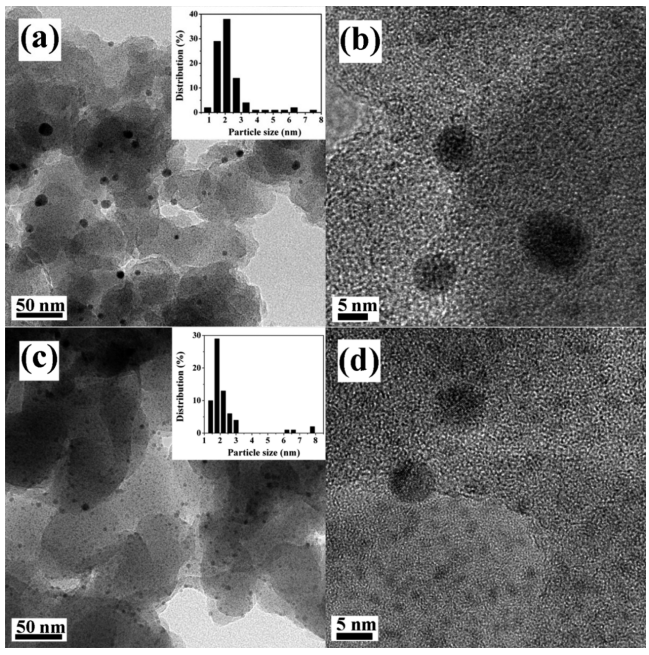

Figure 5. TEM images for Pd@CPP-C after the fourth run (a, b), and Pd@CPP-Y after the seventh run (c, d).

DOI: 10.1021/cs501731w
ACS Catal. 2015, 5, 948−955

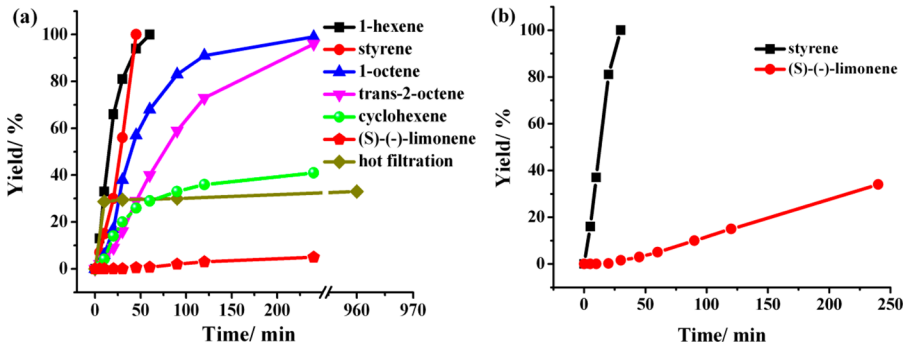

Figure 6. Kinetic profiles for hydrogenation of olefins (a) and hydrogenation of mixture of styrene and (*S*)-(−)-limonene (b) catalyzed by Pd@CPP-Y. Reaction conditions: the molar ratio of olefin to Pd is 5000, 1.0 atm of H_2, 25 °C.

surface NPs through Ostwald ripening.[74] However, palladium NPs in the interior cavities can be effectively restricted by the confinement interaction of the polymer backbone and the coordination interaction between 1,2,3-triazoyl and palladium NPs. In comparison with Pd@CPP-C, Pd@CPP-Y exhibits more restriction against NPs aggregation and superior catalytic activity, which are ascribed to its relatively higher surface area and larger pore volume. It should be mentioned that no catalytic activity was detected when the control experiment for hydrogenation of 1-hexene was performed in the presence of CPP-Y, suggesting that the palladium NPs are crucial for smooth implement of hydrogenation. XPS analyses show that Pd/N molar ratios of fresh Pd@CPP-C and Pd@CPP-Y are 0.048 and 0.071, respectively, whereas Pd/N molar ratios of the used Pd@CPP-C and Pd@CPP-Y are 0.056 and 0.076, respectively, which are slightly higher than that of their respective fresh samples.[75] The increments are possibly ascribed to the migration of palladium from the interior pore to the surface of polymers during hydrogenation, which are consistent with the results of TEM analysis.

To further investigate catalytic performances of Pd@CPP-Y, other olefins were tested. As shown in Figure 6a, complete conversion of 1-octene was achieved in 4 h, which was much slower than that of 1-hexene, suggesting that the reactivity of olefins was significantly affected by the chain length of alkenes. Hydrogenation rate of *trans*-2-octene was slower than 1-octene because of its steric hindrance. Similar to hydrogenation of 1-hexene, hydrogenation of styrene to ethylbenzene also gave a full conversion in 30 min, which probably resulted from $\pi-\pi$ interactions between styrene and aromatic framework of POPs as well as the coordination of styrene to the accessible surface of ultrafine palladium NPs.[76] However, when cyclohexene was employed as a substrate, 30% yield of cyclohexane was achieved in 1 h and was only increased to 40% in 4 h, which was much lower than that of 1-hexene. Interestingly, 2-norbornene was fully hydrogenated in 2 h, which was much faster than cyclohexene, probably because of relatively small bond angle of double bond and considerable strain in the skeleton of 2-norbornene.[77−79] However, hydrogenation of (*S*)-(−)-limonene only gave 5% conversion after 4 h, probably because its large size is unfavorable to access active sites of palladium NPs inside cavity of the polymers. The competition reactions were also performed using a mixture of equimolar styrene and (*S*)-(−)-limonene as substrates. In comparison with hydrogenation of neat styrene and (*S*)-(−)-limonene, a full conversion of styrene was also observed in 30 min, whereas the conversion of (*S*)-(−)-limonene was increased from 5 to 34% after 4 h (Figure 6b). The increment occurred after a nearly full conversion of styrene to ethylbenzene, which is probably attributed to the fact that the swelling behavior of surface pores in Pd@CPP-Y in the presence of ethylbenzene enables (*S*)-(−)-limonene to enter into the pores of polymer and ultimately promotes the contact between (*S*)-(−)-limonene and active sites in polymers.[24,80,81]

It is known that palladium particles in Pd@C are located on the outer surface of carbon, and catalytic reactions occur on the surface of Pd@C. The control experiments of hydrogenation of 1-hexene and 1-octene were investigated using commercial Pd@C. The kinetic profile showed that hydrogenation of 1-octene was slightly slower than 1-hexene in the presence of Pd@C (Figure S9), which was similar to those from Pd@CPP-Y. In comparison with Pd@CPP-Y, Pd@C showed a slightly lower catalytic activity in hydrogenation of 1-hexene, but the catalytic activity in hydrogenation of 1-octene was slightly higher, suggesting that the dispersion of palladium NPs and the property of supports have important effects on hydrogenation of olefins.[82]

To confirm hydrogenation of olefins was indeed catalyzed by palladium NPs in the polymer backbone instead of the leached palladium species, hot filtration and the three-phase test were performed. After hydrogenation of 1-hexene was run for 10 min, Pd@CPP-Y was removed from the reaction mixture by filtration, and the filtrate was allowed to react for 4 h; negligible changes in conversion and selectivity were observed (Figure 6a). ICP analysis of the filtrate shows that palladium leaching is 0.12 ppm, which is insignificant with respect to 0.65 mmol g^{-1} of fresh Pd@CPP-Y. The three-phase test is usually considered to be a useful proof for the detection of homogeneously catalytic active metal species.[83,84] The three-phase test was conducted using Merrifield resin-supported (O-linked) 1-hexenol as an alkene substrate.[52] After hydrogenation, Pd@CPP-Y can be facilely separated from Merrifield resin by centrifugation (Figure S10), and no obvious conversion of resin-bound substrate was observed (Figure 7).

It is known that viscosity of reaction media and physical accessibility of the substrates into the catalytic sites have important effects on hydrogenation of olefins, hydrogenation was also performed in ethanol solution. Pd@CPP-Y showed higher activity than Pd@CPP-C in hydrogenation of 1-hexene (Figure S11), which was consistent with that under solvent-free conditions. Similar variation trends in conversion profiles were observed in hydrogenation of 1-octene, *trans*-2-octene, styrene, and 2-norbornene using Pd@CPP-Y (Figure S12). Besides, the catalytic activities in ethanol were much faster than those under neat conditions. The promotion was mainly ascribed to the decrement of viscosity of olefins in ethanol solution,

DOI: 10.1021/cs501731w
ACS Catal. 2015, 5, 948−955

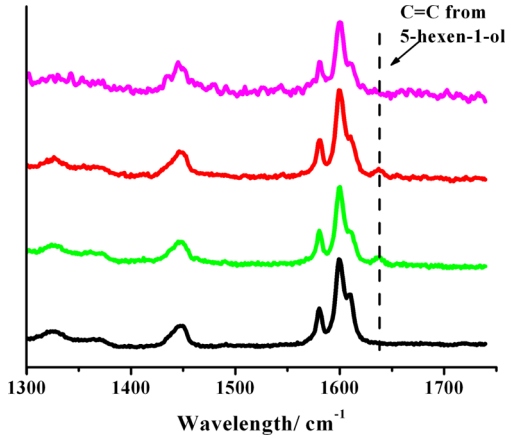

Figure 7. Raman spectra of Merrifield resin (black), 5-hexen-1-ol supported on Merrifield resin (green), attempted hydrogenation of 5-hexen-1-ol supported on Merrifield resin by Pd@CPP-Y (red), 1-hexanol supported on Merrifield resin (purple).

accelerating the accessibility of the catalytically active sites to olefin molecules.

4. CONCLUSIONS

CPP-C and CPP-Y containing 1,2,3-triazolyl linkages have been prepared by click reaction and Yamamoto coupling reaction, respectively. Their structures and properties can be finely tuned by proper choice of synthetic methods. Ultrafine palladium NPs with uniform distribution are facilely incorporated inside the pores of CPP-C and CPP-Y. The confinement interaction of the polymer backbone in conjunction with coordination interaction between 1,2,3-triazoyl and palladium NPs result in good stabilization of palladium NPs. Both Pd@CPP-C and Pd@CPP-Y exhibit excellent catalytic activities in hydrogenation of olefins. Pd@CPP-Y presents higher catalytic activity and recyclability than Pd@CPP-C. In summary, this study not only expands the library of click-based POPs but also provides a useful strategy for the construction of new POP-based catalytic systems with tunable reactivity and stability.

■ ASSOCIATED CONTENT

Supporting Information

The following file is available free of charge on the ACS Publications website at DOI: 10.1021/cs501731w.

Details of the preparation and characterization of materials and NMR spectra for catalytic products (PDF)

■ AUTHOR INFORMATION

Corresponding Author

*E-mail: ruihu@fjirsm.ac.cn.

Notes

The authors declare no competing financial interest.

■ ACKNOWLEDGMENTS

The authors acknowledge 973 Program (2011CBA00502), National Natural Science Foundation of China (21273239, 21471151, 21403238), and Major Project of Fujian Province (2014H0053).

■ REFERENCES

(1) Zaera, F. *Chem. Soc. Rev.* **2013**, *42*, 2746−2762.
(2) Kim, B. H.; Hackett, M. J.; Park, J.; Hyeon, T. *Chem. Mater.* **2014**, *26*, 59−71.
(3) Li, Z.; Liu, J.; Xia, C.; Li, F. *ACS Catal.* **2013**, 2440−2448.
(4) Kibata, T.; Mitsudome, T.; Mizugaki, T.; Jitsukawa, K.; Kaneda, K. *Chem. Commun.* **2013**, *49*, 167−169.
(5) Qiao, B.; Wang, A.; Yang, X.; Allard, L. F.; Jiang, Z.; Cui, Y.; Liu, J.; Li, J.; Zhang, T. *Nat. Chem.* **2011**, *3*, 634−641.
(6) Joo, S. H.; Park, J. Y.; Tsung, C. K.; Yamada, Y.; Yang, P.; Somorjai, G. A. *Nat. Mater.* **2009**, *8*, 126−131.
(7) Myers, V. S.; Weir, M. G.; Carino, E. V.; Yancey, D. F.; Pande, S.; Crooks, R. M. *Chem. Sci.* **2011**, *2*, 1632−1646.
(8) Zhu, Q. L.; Li, J.; Xu, Q. *J. Am. Chem. Soc.* **2013**, *135*, 10210−10213.
(9) Aijaz, A.; Karkamkar, A.; Choi, Y. J.; Tsumori, N.; Ronnebro, E.; Autrey, T.; Shioyama, H.; Xu, Q. *J. Am. Chem. Soc.* **2012**, *134*, 13926−13929.
(10) Lu, G.; Li, S.; Guo, Z.; Farha, O. K.; Hauser, B. G.; Qi, X.; Wang, Y.; Wang, X.; Han, S.; Liu, X. *Nat. Chem.* **2012**, *4*, 310−316.
(11) Khajavi, H.; Stil, H. A.; Kuipers, H. P. C. E.; Gascon, J.; Kapteijn, F. *ACS Catal.* **2013**, *3*, 2617−2626.
(12) Roberts, J. M.; Fini, B. M.; Sarjeant, A. A.; Farha, O. K.; Hupp, J. T.; Scheidt, K. A. *J. Am. Chem. Soc.* **2012**, *134*, 3334−3337.
(13) Saha, D.; Sen, R.; Maity, T.; Koner, S. *Langmuir* **2013**, *29*, 3140−3151.
(14) Kaur, P.; Hupp, J. T.; Nguyen, S. T. *ACS Catal.* **2011**, *1*, 819−835.
(15) Zhang, P.; Weng, Z.; Guo, J.; Wang, C. *Chem. Mater.* **2011**, *23*, 5243−5249.
(16) Hasell, T.; Wood, C. D.; Clowes, R.; Jones, J. T. A.; Khimyak, Y. Z.; Adams, D. J.; Cooper, A. I. *Chem. Mater.* **2010**, *22*, 557−564.
(17) Zhang, Q.; Yang, Y.; Zhang, S. *Chem.—Eur. J.* **2013**, *19*, 10024−10029.
(18) Chan-Thaw, C. E.; Villa, A.; Prati, L.; Thomas, A. *Chem.—Eur. J.* **2011**, *17*, 1052−1057.
(19) Zhou, Y.; Xiang, Z.; Cao, D.; Liu, C. J. *Chem. Commun.* **2013**, *49*, 5633−5635.
(20) Chan-Thaw, C. E.; Villa, A.; Katekomol, P.; Su, D.; Thomas, A.; Prati, L. *Nano Lett.* **2010**, *10*, 537−541.
(21) Dalapati, S.; Jin, S.; Gao, J.; Xu, Y.; Nagai, A.; Jiang, D. *J. Am. Chem. Soc.* **2013**, *135*, 17310−17313.
(22) Fang, Q.; Gu, S.; Zheng, J.; Zhuang, Z.; Qiu, S.; Yan, Y. *Angew. Chem., Int. Ed.* **2014**, *53*, 2878−2882.
(23) Cho, H. C.; Lee, H. S.; Chun, J.; Lee, S. M.; Kim, H. J.; Son, S. U. *Chem. Commun.* **2011**, *47*, 917−919.
(24) Suresh, V. M.; Bonakala, S.; Atreya, H. S.; Balasubramanian, S.; Maji, T. K. *ACS Appl. Mater. Interfaces* **2014**, *6*, 4630−4637.
(25) Wang, W.; Zheng, A.; Zhao, P.; Xia, C.; Li, F. *ACS Catal.* **2014**, *4*, 321−327.
(26) Xu, Y.; Jiang, D. *Chem. Commun.* **2014**, *50*, 2781−2783.
(27) Lu, W.; Wei, Z.; Yuan, D.; Tian, J.; Fordham, S.; Zhou, H. C. *Chem. Mater.* **2014**, *26*, 4589−4597.
(28) Chaikittisilp, W.; Sugawara, A.; Shimojima, A.; Okubo, T. *Chem. Mater.* **2010**, *22*, 4841−4843.
(29) Smith, B. J.; Dichtel, W. R. *J. Am. Chem. Soc.* **2014**, *136*, 8783−8789.
(30) Li, L.; Zhao, H.; Wang, J.; Wang, R. *ACS Nano* **2014**, *8*, 5352−5364.
(31) Bhunia, M. K.; Das, S. K.; Pachfule, P.; Banerjee, R.; Bhaumik, A. *Dalton Trans.* **2012**, *41*, 1304−1311.
(32) Du, X.; Sun, Y. L.; Tan, B. E.; Teng, Q. F.; Yao, X. J.; Su, C. Y.; Wang, W. *Chem. Commun.* **2010**, *46*, 970−972.
(33) Chun, J.; Kang, S.; Kang, N.; Lee, S. M.; Kim, H. J.; Son, S. U. *J. Mater. Chem. A* **2013**, *1*, 5517−5523.
(34) Ding, S. Y.; Gao, J.; Wang, Q.; Zhang, Y.; Song, W. G.; Su, C. Y.; Wang, W. *J. Am. Chem. Soc.* **2011**, *133*, 19816−19822.
(35) Yang, X.; Yao, S.; Yu, M.; Jiang, J. X. *Macromol. Rapid Commun.* **2014**, *35*, 834−839.

DOI: 10.1021/cs501731w
ACS Catal. 2015, 5, 948−955

(36) Liang, L.; Astruc, D. *Coord. Chem. Rev.* **2011**, *255*, 2933−2945.
(37) Barner-Kowollik, C.; Du Prez, F. E.; Espeel, P.; Hawker, C. J.; Junkers, T.; Schlaad, H.; Van Camp, W. *Angew. Chem., Int. Ed.* **2011**, *50*, 60−62.
(38) Kolb, H. C.; Finn, M. G.; Sharpless, K. B. *Angew. Chem., Int. Ed.* **2001**, *40*, 2004−2021.
(39) Holst, J. R.; Stöckel, E.; Adams, D. J.; Cooper, A. I. *Macromolecules* **2010**, *43*, 8531−8538.
(40) Pandey, P.; Farha, O. K.; Spokoyny, A. M.; Mirkin, C. A.; Kanatzidis, M. G.; Hupp, J. T.; Nguyen, S. T. *J. Mater. Chem.* **2011**, *21*, 1700−1703.
(41) Xie, L. H.; Suh, M. P. *Chem.—Eur. J.* **2013**, *19*, 11590−11597.
(42) Plietzsch, O.; Schilling, C. I.; Grab, T.; Grage, S. L.; Ulrich, A. S.; Comotti, A.; Sozzani, P.; Muller, T.; Brase, S. *New J. Chem.* **2011**, *35*, 1577−1581.
(43) Dawson, R.; Stöckel, E.; Holst, J. R.; Adams, D. J.; Cooper, A. I. *Energy Environ. Sci.* **2011**, *4*, 4239−4245.
(44) Zhong, H.; Gong, Y.; Zhang, F.; Li, L.; Wang, R. *J. Mater. Chem. A* **2014**, *2*, 7502−7508.
(45) Wu, H.; Li, H.; Kwok, R. T.; Zhao, E.; Sun, J. Z.; Qin, A.; Tang, B. Z. *Sci. Rep.* **2014**, *4*, 5107.
(46) Schmidt, J.; Werner, M.; Thomas, A. *Macromolecules* **2009**, *42*, 4426−4429.
(47) Ben, T.; Pei, C.; Zhang, D.; Xu, J.; Deng, F.; Jing, X.; Qiu, S. *Energy Environ. Sci.* **2011**, *4*, 3991−3999.
(48) Lu, W.; Yuan, D.; Zhao, D.; Schilling, C. I.; Plietzsch, O.; Muller, T.; Bräse, S.; Guenther, J.; Blümel, J.; Krishna, R.; Li, Z.; Zhou, H. C. *Chem. Mater.* **2010**, *22*, 5964−5972.
(49) Jiang, J. X.; Trewin, A.; Adams, D. J.; Cooper, A. I. *Chem. Sci.* **2011**, *2*, 1777−1781.
(50) Zhang, Q.; Zhang, S. B.; Li, S. H. *Macromolecules* **2012**, *45*, 2981−2988.
(51) Xiang, Z.; Zhou, X.; Zhou, C.; Zhong, S.; He, X.; Qin, C.; Cao, D. *J. Mater. Chem.* **2012**, *22*, 22663−22669.
(52) Zhang, C.; Liu, Y.; Li, B.; Tan, B.; Chen, C. F.; Xu, H. B.; Yang, X. L. *ACS Macro Lett.* **2012**, *1*, 190−193.
(53) Ben, T.; Ren, H.; Ma, S.; Cao, D.; Lan, J.; Jing, X.; Wang, W.; Xu, J.; Deng, F.; Simmons, J. M.; Qiu, S.; Zhu, G. *Angew. Chem., Int. Ed.* **2009**, *48*, 9457−9460.
(54) Yuan, D.; Lu, W.; Zhao, D.; Zhou, H. C. *Adv. Mater.* **2011**, *23*, 3723−3725.
(55) Campbell-Verduyn, L. S.; Mirfeizi, L.; Dierckx, R. A.; Elsinga, P. H.; Feringa, B. L. *Chem. Commun.* **2009**, 2139−2141.
(56) Leininger, S.; Stang, P. J.; Huang, S. P. *Organometallics* **1998**, *17*, 3981−3987.
(57) Genna, D. T.; Wong-Foy, A. G.; Matzger, A. J.; Sanford, M. S. *J. Am. Chem. Soc.* **2013**, *135*, 10586−10589.
(58) Devadoss, A.; Chidsey, C. E. *J. Am. Chem. Soc.* **2007**, *129*, 5370−5371.
(59) Bebensee, F.; Bombis, C.; Vadapoo, S. R.; Cramer, J. R.; Besenbacher, F.; Gothelf, K. V.; Linderoth, T. R. *J. Am. Chem. Soc.* **2013**, *135*, 2136−2139.
(60) Arab, P.; Rabbani, M. G.; Sekizkardes, A. K.; İslamoğlu, T.; El-Kaderi, H. M. *Chem. Mater.* **2014**, *26*, 1385−1392.
(61) Weber, J.; Schmidt, J.; Thomas, A.; Bohlmann, W. *Langmuir* **2010**, *26*, 15650−15656.
(62) Cárdenas-Lizana, F.; Berguerand, C.; Yuranov, I.; Kiwi-Minsker, L. *J. Catal.* **2013**, *301*, 103−111.
(63) Ornelas, C.; Aranzaes, J. R.; Salmon, L.; Astruc, D. *Chem.—Eur. J.* **2008**, *14*, 50−64.
(64) Liang, Q.; Liu, J.; Wei, Y.; Zhao, Z.; MacLachlan, M. J. *Chem. Commun.* **2013**, *49*, 8928−8930.
(65) Martis, M.; Mori, K.; Fujiwara, K.; Ahn, W.-S.; Yamashita, H. *J. Phys. Chem. C* **2013**, *117*, 22805−22810.
(66) Yuan, B.; Pan, Y.; Li, Y.; Yin, B.; Jiang, H. *Angew. Chem., Int. Ed.* **2010**, *49*, 4054−4058.
(67) Saha, D.; Deng, S. *Langmuir* **2009**, *25*, 12550−12560.
(68) Park, I. H.; Medishetty, R.; Lee, S. S.; Vittal, J. J. *Chem. Commun.* **2014**, *50*, 6585−6588.
(69) Vajda, S.; Pellin, M. J.; Greeley, J. P.; Marshall, C. L.; Curtiss, L. A.; Ballentine, G. A.; Elam, J. W.; Catillon-Mucherie, S.; Redfern, P. C.; Mehmood, F. *Nat. Mater.* **2009**, *8*, 213−216.
(70) Mondal, A.; Jana, N. R. *ACS Catal.* **2014**, *4*, 593−599.
(71) Sabo, M.; Henschel, A.; Froede, H.; Klemm, E.; Kaskel, S. *J. Mater. Chem.* **2007**, *17*, 3827−3832.
(72) Sadeghmoghaddam, E.; Gu, H.; Shon, Y.-S. *ACS Catal.* **2012**, *2*, 1838−1845.
(73) Wilde, M.; Fukutani, K.; Ludwig, W.; Brandt, B.; Fischer, J. H.; Schauermann, S.; Freund, H. J. *Angew. Chem., Int. Ed.* **2008**, *47*, 9289−9293.
(74) Ishiwata, T.; Furukawa, Y.; Sugikawa, K.; Kokado, K.; Sada, K. *J. Am. Chem. Soc.* **2013**, *135*, 5427−5432.
(75) Long, W.; Brunelli, N. A.; Didas, S. A.; Ping, E. W.; Jones, C. W. *ACS Catal.* **2013**, *3*, 1700−1708.
(76) Kelsen, V.; Wendt, B.; Werkmeister, S.; Junge, K.; Beller, M.; Chaudret, B. *Chem. Commun.* **2013**, *49*, 3416−3418.
(77) Choudary, B. M.; Lakshmi Kantam, M.; Mahender Reddy, N.; Koteswara Rao, K.; Haritha, Y.; Bhaskar, V.; Figueras, F.; Tuel, A. *Appl. Catal. A: Gen.* **1999**, *181*, 139−144.
(78) Niederer, J. P. M.; Arnold, A. B. J.; Hölderich, W. F.; Spliethof, B.; Tesche, B.; Reetz, M.; Bönnemann, H. *Top. Catal.* **2002**, *18*, 265−269.
(79) Lopez, S. A.; Houk, K. N. *J. Org. Chem.* **2013**, *78*, 1778−1783.
(80) Rao, K. V.; Mohapatra, S.; Maji, T. K.; George, S. J. *Chem.—Eur. J.* **2012**, *18*, 4505−4509.
(81) Roy, S. G.; Haldar, U.; De, P. *ACS Appl. Mater. Interfaces* **2014**, *6*, 4233−4241.
(82) Niu, Y.; Yeung, L. K.; Crooks, R. M. *J. Am. Chem. Soc.* **2001**, *123*, 6840−6846.
(83) Crudden, C. M.; Sateesh, M.; Lewis, R. *J. Am. Chem. Soc.* **2005**, *127*, 10045−10050.
(84) Phan, N. T. S.; Van Der Sluys, M.; Jones, C. W. *Adv. Synth. Catal.* **2006**, *348*, 609−679.

DOI: 10.1021/cs501731w
ACS Catal. 2015, 5, 948−955